Supporting Information

Enhanced Thermal-to-Flexible Phase Change Materials Based on Cellulose/Modified Graphene Composites for Thermal Management of Solar Energy

Yongqiang Qian[1, 2, 3], Na Han[1, 2, 3, 4]*, Zongxuan Zhang[1, 2, 3], Ruirui Cao[1, 2, 3], Linli Tan[1, 2, 3], Wei Li[1, 2, 3], Xingxiang Zhang[1, 2, 3]*

[1]State Key Laboratory of Separation Membranes and Membrane Processes, Tianjin 300387, China

[2]Tianjin Municipal Key Lab of Advanced Fiber and Energy Storage Technology, Tianjin 300387, China

[3]School of Material Science and Engineering, Tiangong University, Tianjin 300387, China

[4]Department of Textile Engineering, Chemistry & Science, College of Textiles, North Carolina State University, Raleigh, North Carolina 27695, United States

Corresponding Author

*E-mail: hannatjpu@gmail.com; zhangpolyu@aliyun.com.

Preparation of initiator-modified cellulose 2-bromopropionylate (Cell-Br)

Cellulose (1.25 g, 7.72 mmol) was suspended in 24 mL of anhydrous DMAc and stirred at 120 °C for 1 h. The slurry was then cooled to 100 °C, and LiCl (3 g, 70.8 mmol) was added and stirred for another 30 min. The mixture was cooled to room temperature and kept stable overnight. BPB (3.5 g, 38.7 mmol) was dropwised to the homogeneous solution in an ice/water bath. When the dropping process was completed, the reaction mixture was left to room temperature. After 4 h, the solution was heated to 50 °C and stirred for 2 h. The reaction mixture was allowed to cool to room temperature, and the polymer was isolated by precipitation in ethanol. Further purification was achieved by the re-dissolution of the crude product in 60 mL of acetone and re-precipitation in ethanol to produce a white powder. The resulting product was dried in vacuum at 50 °C. The obtained yield is 72 wt.%.

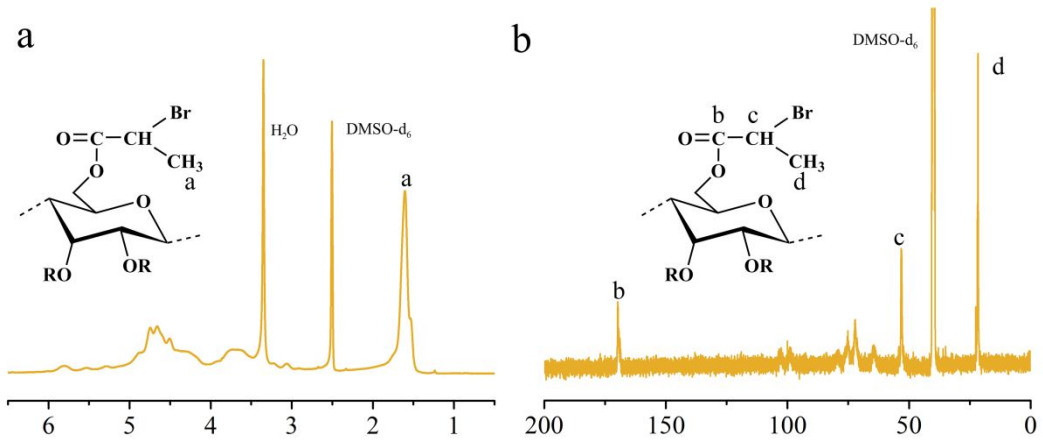

Figure S1. (a) ^{1}H NMR and (b) ^{13}C NMR spectra of Cell-Br.

The resulting ^{1}H NMR spectrum (Figure S1a) shows a peak at δ = 1.59 ppm that is attributed to the methyl protons of the bromopropionyl group in Cell-Br, with a substitution degree of 1.75. Meanwhile, the chemical shift at 170 ppm in the ^{13}C NMR spectrum (Figure S1b) confirms the presence of the carbonyl group. The peaks

corresponding to methyl and methenyl carbon atoms appear at 22 and 53 ppm, respectively. However, a comparison of the FTIR spectra of cellulose and Cell-Br (Figure 2d) clearly shows that the intensity of the hydroxyl group band in the former decreases upon reaction with 2-bromopropionyl bromide. This is probably due to the substitution of some cellulosic hydroxyl groups by propionyl groups. The new peaks appearing at 1752 cm^{-1} and 703 cm^{-1} in the Cell-Br FT-IR spectrum are attributed to the carbonyl and bromo groups, respectively. Overall, the spectroscopic analyses confirm the successful preparation of the initiator-modified cellulose, Cell-Br.

Preparation of modified GN nanosheets (GN16)

Modified GN, denoted by GN16, was synthetized according to the following procedure. First, 1 g of GN was dispersed in DMAc by ultrasonication for 2 h. Subsequently, HQ inhibitor was added to the uniform suspension, followed by the slow dropping of 15 g of A16 (50 mmol). The solution was continually mixed at 180°C under nitrogen atmosphere. 12 h later, the GN16 product was filtered and rinsed extensively with tetrahydrofuran (THF), then it was dried and stored for subsequent use.

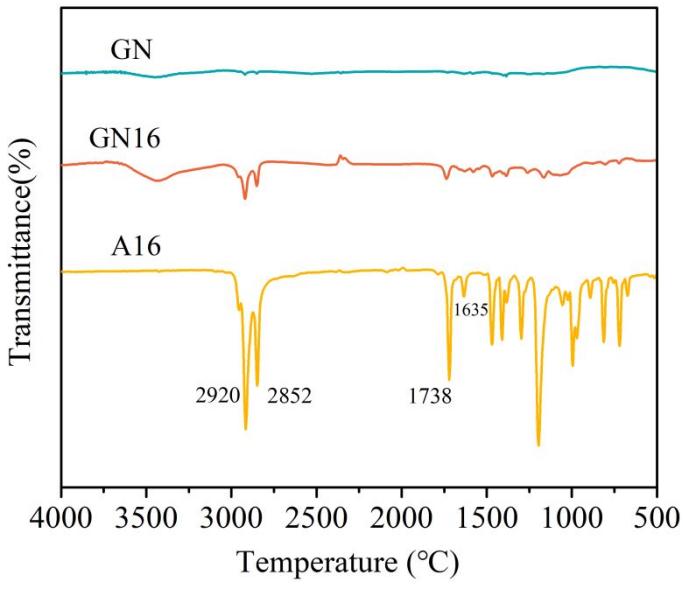

Figure S2. FT-IR spectra of GN, A16 and GN16

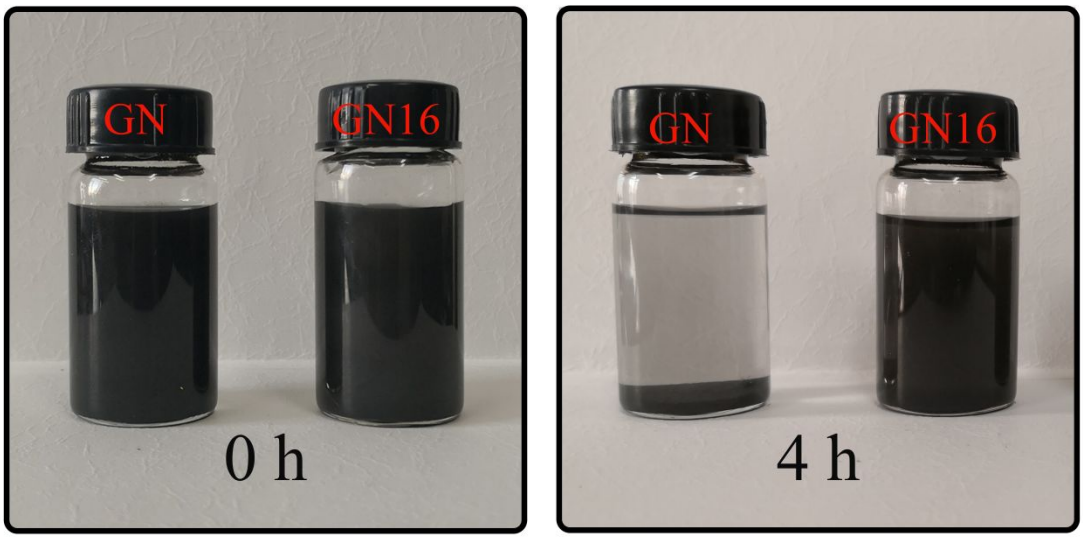

Figure S3 The dispersibility of GN and GN16 in DMAc after 4 h standing.

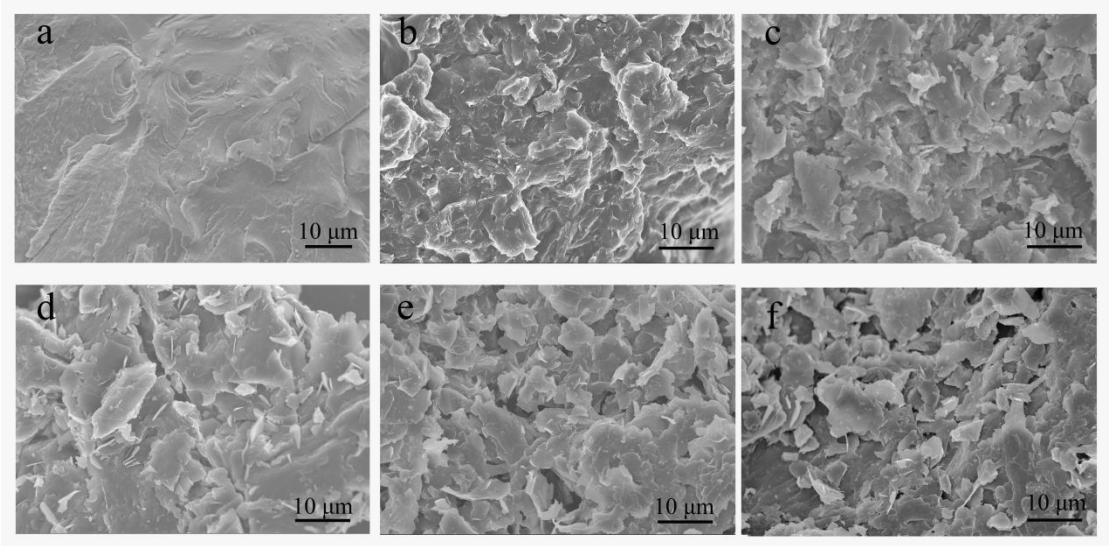

Figure S4. SEM images of CP (a), CPmG-1 (b), CPmG-3 (c), CPmG-5 (d), CPmG-7 (e) and CPmG-9 (f).

Table S1. X-ray diffractometry data

Sample	2θ		d_{110} (nm)	d_{002} (nm)
	110	002		
GN	-	26.48	-	0.336
GN16	21.62	26.68	0.410	0.334
PA16	21.50	-	0.412	-
CP	21.35	-	0.415	-
CPmG-1	21.44	26.50	0.413	0.336
CPmG-3	21.46	26.54	0.413	0.336
CPmG-5	21.45	26.62	0.413	0.334
CPmG-7	21.44	26.74	0.413	0.332
CPmG-9	21.40	26.50	0.414	0.336

Table S2. Crystalline properties of PA16 and CPmG-x from DSC analysis

Specimen	GN16 (%)	ΔH_m (J/g)	X_c (%)	n_c
PA16	-	93	32.8	6.9
CP	0	77	27.2	5.7
CPmG-1	1	87	30.7	6.5
CPmG-3	3	96	33.9	7.2
CPmG-5	5	103	36.3	7.7
CPmG-7	7	90	31.7	6.7
CPmG-9	9	78	27.3	5.8

The crystallinity (X_c) of the synthesized SSPCMs and the number of crystallized CH_2 and CH_3 groups (n_c) in the side chains of PA16, CP, and CPmG-x materials were calculated according to equations (S1) and (S2), respectively:

$$X_C = \frac{\Delta H_m(n) \times 14.026}{C + k(n)} \qquad (S1)$$

$$n_c = \frac{\Delta H_m \times M_{unit}}{k} \quad \text{(S2)}$$

Where n is the number of methylene and methyl groups in the side chains, and M_{unit} is the relative molecular mass of the structural unit of the phase change working substance (296.49 g mol^{-1}).[1] C and k values are zero and 3971 J mol^{-1}, respectively.[2, 3]

The calculated values listed in Table S2 show that the macro-fluidity of PA16 is greatly impeded upon grafting onto the cellulose support due to the restriction of the free movement of side chains, even at temperatures higher than the melting point. Accordingly, the X_c and n_c of CP are significantly less than the corresponding values of PA16. However, X_c and n_c are gradually enhanced upon the incorporation of up to 5% GN16 into CP. The X_c of material containing 5% dispersed GN16 is greater than both, the CP (9.1% greater) and pure PA16 values, which signifies that the incorporation of GN16 into the material increases the number of CH_2 groups in the crystal lattice. Therefore, it may be concluded that GN16 promotes alkyl chain crystallization, resulting in higher n_c values. Increasing the GN16 content beyond 5% results in the gradual decrease of X_c and n_c values in CPmG-x. This is due to the restriction of side chain free movement by excessive GN16, which ultimately leads to reduced enthalpy of the material.

Table S3. Thermal stabilities of GN, GN16, Cell-Br, CP and CPmG-x

Sample No.	Ta do (°C)	Tb dp (°C)	Mass loss (%)
GN	-	-	0
GN16	341	369	15
Cell-Br	277	290	85
CP	299	407	96
CPmG-1	376	408	92
CPmG-3	375	408	91
CPmG-5	370	406	90
CPmG-7	372	406	89
CPmG-9	368	406	87

[a]: The onset decomposition temperature; [b]: The fastest decomposition temperature.

Shape stabilization performance and thermal reliability behavior

Shape-stabilized test of SSPCMs was realized by visual observation method. For direct observation, the pressed PA16, CP, and CPmG-x with a diameter 20 mm and 7.5 mm in thickness was put into a 60°C oven for 30 min, and then recorded the changes of disc size and morphology. Additionally, Thermal reliability of 100 heating/cooling cycles was conducted by a programmable controller (Giant Force) with temperature changing from 0 to 100°C. After that, the thermal reliability and the structural stability were determined by DSC and FT-IR analysis before and after 100 heating/cooling cycles.

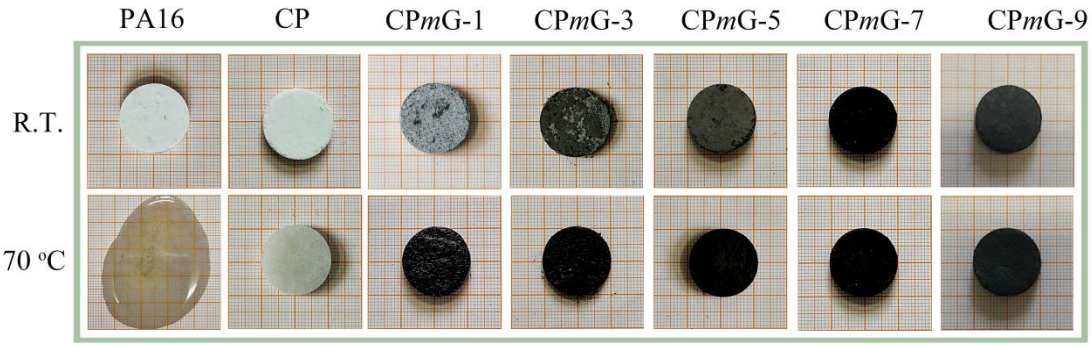

Figure S5. Shape-stability of PA16, CP and CPmG-x with respect to temperature through the visual observation

The leakage and flowability of solid-liquid PCMs in melting state is the biggest barrier for practical applications. Here, leakage tests for CPmG-x are performed in hot stage at 70°C for 10 min. The thermal behavior of the thermo-responsive samples is observed by a digital camera as shown in Figure S3. For CP, it is a white and opaque wafer due to the crystalline of PA16 at ambient temperature. The sample CP just become semitransparent and changes to an elastomer without any leakage after 10 min heating, implying the melting of side chain PA16 crystals. All thermo-responsive samples CPmG-x are black one for due to the introduction of the GN16. There is no significant change at the macroscopic level and they remained in the solid state. It is proved that the all thermo-responsive CPmG-x composites are the solid-solid phase change materials and have possess outstanding shape stability, implying the melting of PA16 crystals.

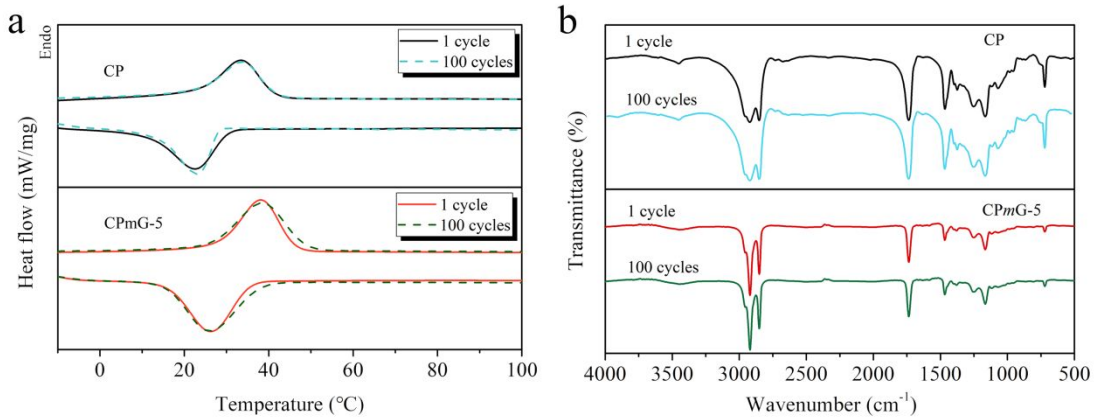

Figure S6. DSC curves (a) and FT-IR spectra (b) of CP and CPmG-5 before and after the 100 thermal cycling treatments.

Thermal reliability and cycling stability of PCMs are crucial points in the area of thermal energy storage (TES) application. Here, taking CP and CPmG-x as an example, the thermal reliability and structural stability are compared before and after 100 times thermal cycles. The DSC and FT-IR results are showed in Figure S4a and b, and the corresponding thermal data is summarized in Table 2. After 100 times thermal cycles, T_m and T_c of CP and CPmG-5 exhibit a 0.3-0.8^{o}C downshift as compared with the ones untreated. Meanwhile, the phase transition enthalpy of CP and CPmG-5 shows a 1-3 J/g decrement, which is negligible for thermal energy storage applications. In Figure S4b, it is shown that there is no obvious change in the structure of the samples after 100 thermal cycles. It is further demonstrated that the SSPCMs have a good structural stability. It could be concluded that the CPmG-x composites can be a good alternative in the area of TES materials.

Table S4. TC of relative polymer composites doped with GN nanofillers in the available literature

Reference	Sample	Dimensions		Filter content (%)	TC (W/mK)
		Size	Thick		
14	Paraffin/GN	N/A		10	0.5
16	Paraffin /xGnP-1	~10 μm	~10 nm	5	0.5
22	Paraffin/xGnP	~15 μm	~10 nm	3	0.454
				5	0.616
24	LA/GO foam	N/A		5	0.91
	LA/GO-LA foam				1.27
40	Epoxy/GNPs	3.9 μm	~100 nm	1.1	0.3
				2.2	0.32
				4.5	0.5
	Epoxy/ modified GNPs			1.1	0.3
				2.2	0.43
				4.5	1.25
Our work	CPmG-1	~10 μm	3-9 nm	1	0.3
	CPmG-3			3	0.49
	CPmG-5			5	0.7
	CPmG-7			7	0.95
	CPmG-9			9	1.32

REFERENCE

(1) Li, J.; Wang, H.-X.; Kong, L.; Zhou, Y.; Li, S.-Q.; Shi, H.-F., Phase transition and side-chain crystallization of poly(methyl vinyl ether-*alt*-maleic anhydride)-g-alkyl alcohol comb-like polymers. *Macromolecules* **2018,** *51*, 8922-8931.

(2) Jordan, E.-F.; Feldeisen, D.-W.; Wrigley, A.-N., Side-chain crystallinity. I. heats of fusion and melting transitions on selected homopolymers having long side chains. *J. Polym. Sci. Part A-1* **1997,** *9*, 1853-1852.

(3) Jin, Y.-M.; Liu, H.-H.; Wang, N.; Hou, L.-C.; Zhang, X.-X., Dispersibility and

chemical bonds between multi-walled carbon nanotubes and poly(ether ether ketone) in nanocomposite fibers. *Mater. Chem. Phys.* **2012,** *135* (2-3), 948-956.